Carbon-13 Relaxation Study of Chain Segmental Motion and Side-Chain Internal Rotations of Poly(isobutyl methacrylate) in Solution

Sapna Ravindranathan and D. N. Sathyanarayana*

Department of Inorganic and Physical Chemistry, Indian Institute of Science, Bangalore 560 012, India

Received August 17, 1995[⊗]

ABSTRACT: The dynamics of poly(isobutyl methacrylate) in toluene solution has been examined by ^{13}C spin−lattice relaxation time and NOE measurements as a function of temperature. The experiments were performed at 50.3 and 100.6 MHz. The backbone carbon relaxation data have been analyzed using the Dejean−Laupretre−Monnerie (DLM) model, which describes the dynamical processes in the backbone in terms of conformational transitions and bond librations. The relaxation data of the side chain nuclei have been analyzed by assuming different motional models, namely, unrestricted rotational diffusion, three site jumps, and restricted rotational diffusion. The different models have been compared for their ability to reproduce the experimental spin−lattice relaxation times and also to predict the behavior of NOE as a function of temperature. Conformational energy calculations have been carried out on a model compound by using the semiempirical quantum chemical method, AM1, and the results confirm the validity of the motional models used to describe the side-chain motion.

Introduction

^{13}C NMR has proved to be a very powerful technique for studying the local dynamics of polymers. The ^{13}C spin−lattice and spin−spin relaxation times (T_1 and T_2) and the nuclear Overhauser enhancements (NOE) are the important experimental quantities for probing the dynamical processes. Since the ^{13}C nucleus is of low natural abundance, the relaxation is dominated by the dipolar interactions with the directly bonded hydrogens. By studying the relaxation of the nuclei in different environments of the chain, it is possible to obtain a detailed picture of the motions occurring in different parts of the chain.

Nuclear magnetic relaxation parameters provide information about the molecular motion through their relationship to the spectral density function which is the Fourier transform of the orientational time correlation function of the relaxing dipoles. The time correlation function embodies the mechanisms and rates of the molecular motions, and obtaining information on this function is the objective of the relaxation studies. The time correlation function is derived on the basis of a specific model of the polymer motion, and with the aid of this function, the measured relaxation data can be used to obtain information about the dynamical processes occurring in different parts of the chain.

The dynamical processes which occur in polymer chains are mainly the rearrangement processes which occur in short segments of the backbone and side-chain motions. There are several models which describe backbone motion in terms of the conformational transitions, and these have been reviewed extensively.[1−3] However, recent studies have shown that more localized motions, namely librations of the C−H vectors of the backbone should also be considered in addition to the conformational transitions, in order to understand the differences in the dynamics of the C−H vectors at different sites of the backbone.[4−6] Several models have been proposed to describe internal motions in the side chains. For alkyl side chains, the models consider multiple internal rotations, involving the dihedral angles along the chain. These motional processes have been modeled as free internal rotations, restricted rotations, and jumps among potential minima.[7−15] For simplicity, these models assume that the various motions are independent.

In the present study, ^{13}C spin−lattice relaxation times (T_1) and nuclear Overhauser enhancements (NOEs) of poly(isobutyl methacrylate) (PIBM) have been measured in toluene solution as a function of temperature at 50 and 100 MHz. For describing the backbone dynamics, we have used the Dejean−Laupretre−Monnerie (DLM) model,[14] which describes the backbone motion in terms of the conformational transitions of short segments of the chain and librations of the C−H vectors on the backbone. The dynamics of the alkyl side chains have been analyzed in terms of different motional models. Further we have carried out conformational energy calculations on a model compound to obtain a more detailed insight into the side-chain motion. These results have been utilized to check the validity of the various motional models for side-chain motion.

Experimental Section

The PIBM sample used in the present study was obtained from Aldrich. Its molecular weight characteristics are M_n = 140 000 and M_w = 300 000. The sample used for NMR experiments was 30% (wt/vol) in toluene d_8.[16]

The ^{13}C nuclear magnetic resonance experiments were carried out on Bruker ACF-200 and Bruker AMX-400 spectrometers operating at 50.3 and 100.6 MHz, respectively, for the ^{13}C nucleus. The sample temperature was regulated to ±1 K. The spin−lattice relaxation times were measured by the inversion recovery technique, which uses a 180°−τ−90° pulse sequence. The delay times between two sequences were 5 times longer than the highest T_1, among those which were to be determined simultaneously. An initial estimate of the T_1 values was obtained from preliminary experiments. A total of 100−200 acquisitions were accumulated for each set of 14 arrayed τ values. The T_1 values were determined by fitting the signal intensities as a function of delay time to a three-parameter exponential function.[17] The nuclear Overhauser enhancements (NOE) were measured by comparing ^{13}C signal intensities of spectra acquired by continuous ^1H decoupling and inverse gated decoupling. In the NOE experiments, delays

[⊗] Abstract published in *Advance ACS Abstracts,* March 15, 1996.

S0024-9297(95)01207-1 CCC: $12.00

of 10 times T_1 were used between the acquisitions. Experiments were performed on undegassed samples, since the relaxation times of interest are less than 4 s and, in such cases, the presence of dissolved oxygen is not expected to contribute significantly to relaxation.[18] The measured T_1 values are accurate to within 8%, and the NOEs, to about 15%.

The labeling scheme of the carbon atoms in the repeating unit of PIBM is indicated below. The ^{13}C NMR relaxation data from carbons C_β, C_1, C_3, and C_4 are analyzed in this paper.

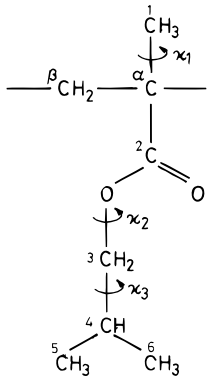

Relaxation Equations

Assuming a purely $^{13}C-^{1}H$ dipolar relaxation mechanism, the expressions for the spin−lattice relaxation time, T_1, and the nuclear Overhauser enhancement, NOE, under conditions of complete proton decoupling are given by[19]

$$\frac{1}{T_1} = \frac{N}{10}\left[\frac{\mu_0 \hbar \gamma_H \gamma_C}{4\pi r^3}\right]^2 [J(\omega_H - \omega_C) + 3J(\omega_C) + 6J(\omega_H + \omega_C)] \quad (1)$$

$$\mathrm{NOE} = 1 + \frac{\gamma_H}{\gamma_C}\left[\frac{6J(\omega_H + \omega_C) - J(\omega_H - \omega_C)}{J(\omega_H - \omega_C) + 3J(\omega_C) + 6J(\omega_H + \omega_C)}\right] \quad (2)$$

where γ_C and γ_H are the magnetogyric ratios of the ^{13}C and ^{1}H nuclei, respectively, μ_0 is the permeability of a vacuum, N is the number of directly bonded protons, r is the C−H internuclear distance, $\hbar = h/2\pi$ where h is Planck's constant, and ω_H and ω_C are the Larmor frequencies of ^{1}H and ^{13}C, respectively. We have used an r value of 1.09 obtained from quantum chemistry for all the C−H distances.[20] Another relaxation mechanism, which becomes important at high magnetic field strengths is the chemical shift anisotropy. However, this mechanism is more important in the case of unsaturated and aromatic carbons, hence we have not included it in the present calculations which involve only aliphatic carbons. The spectral density function, $J(\omega)$, is obtained by the Fourier transformation of the correlation function, $G(t)$.

$$J(\omega) = \frac{1}{2}\int_{-\infty}^{\infty} G(t) e^{i\omega t}\, dt \quad (3)$$

The correlation function is derived on the basis of specific models for polymer motion.

Motional Models

(i) Backbone Motion. Several models have been proposed to describe the local chain dynamics of polymers in solution. Most of these models consider only conformational transitions of short segments of the backbone for describing the dynamical process. Recently, there has been considerable emphasis in the literature on the necessity of considering two classes of motions occurring on well-separated time scales for a better description of the backbone motion, and this was first proposed by Dejean et al.[4] The Dejean, Laupretre, Monnerie (DLM) model is a modification of the Hall−Weber−Helfand (HWH)[21] model, which describes the backbone dynamics in terms of correlated pair transitions involving simultaneous rotations about two bonds and isolated transitions involving rotation about one bond. The HWH model underestimates the value of T_1 at the minimum and it fails to account for the different local dynamics observed at different carbons of the polymer backbone. The DLM model overcomes these deficiencies by superimposing an additional independent motion on the backbone rearrangement of the HWH model. The additional motion involves librations of the C−H vectors of the backbone. The DLM spectral density function is given by

$$J(\omega) = \frac{1 - f}{(\alpha + i\beta)^{1/2}} + \frac{f\tau_1}{1 + \omega^2 \tau_1^2} \quad (4)$$

where

$$\alpha = \frac{1}{\tau_0^2} + \frac{2}{\tau_0 \tau_1} - \omega^2 \quad (5)$$

and

$$\beta = -2\omega\left[\frac{1}{\tau_0} + \frac{1}{\tau_1}\right] \quad (6)$$

Here, τ_l is the correlation time for libration, f is the relative weight of the librational component, and τ_1 and τ_0 are the correlation times for the pair and isolated transitions, respectively.

(ii) Side-Chain Motion. The relaxation of the nuclei in the side chains is governed by the conformational transitions of the backbone and rotational motions of the side groups, which result in the reorientation of the C−H vectors. The conformational transitions of the backbone are described by the term proportional to the factor $(1 - f)$ in eq 4, and it corresponds to the spectral density function of the HWH model.

Various models have been proposed to describe the multiple internal rotations in the side chains. Woessner has treated the case of a molecule with an internal rotation about only one bond. The two models assumed were jumps among three equivalent sites and unrestricted rotational diffusion.[13] The latter model has been extended to the case of molecules with long side chains undergoing multiple internal motions.[8] London and Avitabile[11] have treated the problem of multiple internal rotations by assuming that the rotational diffusion is limited to a restricted angular range. Conformational constraints resulting from steric interactions within the side chain and the polymer backbone are assumed to result in restricted rotations. An equivalent result has been obtained by Wittebort and Szabo[10] for restricted rotational motion of side chains. However, the spectral density function obtained by Wittebort and Szabo has an extra factor involving the Euler angle, α, for the case of successive internal rotations. Apart from this factor, the spectral density expression obtained for both the models are the same.

In the present study, internal motions occurring in the side chains have been modeled as unrestricted rotational diffusion, restricted rotational diffusion, or three site jumps. For the three site jump motions, we follow the approach of Woessner[13] and for the restricted rotational diffusion, we follow the approach of London and Avitabile.[11] The models considered for the specific motions and the corresponding expressions for the spectral density are given below.

The following models have been considered for the internal motion of the α-methyl side group, which is indicated as χ_1 motion in the labeling scheme.

(1) Unrestricted rotational diffusion model[7,8] for which the composite spectral density function is given by

$$J(\omega) = \sum_{b=-2}^{2} [d^{(2)}_{b0}(\beta_{1F})]^2 \, \mathrm{Re}\left[\frac{1}{(\alpha' + i\beta')^{1/2}}\right] \qquad (7)$$

Here, α' and β' are obtained by replacing τ_0^{-1} in eqs 5 and 6 by $\tau_0^{-1} + b^2D$, where D is the diffusion constant for the rotation of the methyl group. The functions $d^{(2)}_{b0}(\beta_{1F})$ are elements of the reduced Wigner rotation matrices,[22] β_{1F} being the angle between the rotation axis and the internuclear C−H vector.

(2) Three site jump model[13] with equal populations and correlation time τ_{ir}, in which case the spectral density is given by

$$J(\omega) = \frac{1}{4}[3\cos^2\beta_{1F} - 1]^2 \, \mathrm{Re}\left[\frac{1}{(\alpha + i\beta)^{1/2}}\right] + \frac{3}{4}[\sin^2 2\beta_{1F} + \sin^4\beta_{1F}] \, \mathrm{Re}\left[\frac{1}{(\alpha' + i\beta')^{1/2}}\right] \qquad (8)$$

The α' and β' of eq 8 are obtained by replacing τ_0^{-1} in eqs 5 and 6 by $\tau_0^{-1} + \tau_{ir}^{-1}$.

(3) Restricted rotational diffusion[11] with spectral density function,

$$J(\omega) = \sum_{n=0}^{\infty} \sum_{b=-2}^{2} [d^{(2)}_{b0}(\beta_{1F})]^2 E(b,n)^2 \, \mathrm{Re}\left[\frac{1}{(\alpha' + i\beta')^{1/2}}\right] \qquad (9)$$

The α' and β' of eq 9 are obtained by replacing τ_0^{-1} in eqs 5 and 6 by

$$\tau_0^{-1} + \left(\frac{n\pi}{2\gamma}\right)^2 D$$

Here, γ is the angular amplitude of the rotation. $E(b,n)$ is a function of the angle γ and is given by

$$E(b,0) = \frac{\sin b\gamma}{b\gamma} \qquad (10)$$

$$E(b,n\neq 0) = \frac{1}{2^{1/2}}\left[\frac{\sin\left(b\gamma - \frac{n\pi}{2}\right)}{b\gamma - \frac{n\pi}{2}} + (-1)^n \frac{\sin\left(b\gamma + \frac{n\pi}{2}\right)}{b\gamma + \frac{n\pi}{2}}\right] \qquad (11)$$

The internal motions considered in the ester side chain are indicated as χ_2 and χ_3 motions in the labeling scheme. In modeling the multiple internal rotations within the ester side chain, we consider the following motions.

(1) Restricted rotational diffusion about χ_2 and unrestricted rotational diffusion about χ_3. The spectral density function is given by

$$J(\omega) = \sum_{n_1=0}^{\infty} \sum_{b_1,b_2=-2}^{2} [d^{(2)}_{b_1b_2}(\beta_{12})]^2 \, E(b_1,n_1)^2 [d^{(2)}_{b_20}(\beta_{2F})]^2 \times \mathrm{Re}\left[\frac{1}{(\alpha' + i\beta')^{1/2}}\right] \qquad (12)$$

The α' and β' are obtained by replacing τ_0^{-1} in eqs 5 and 6 by

$$\tau_0^{-1} + \left(\frac{n\pi}{2\gamma_1}\right)^2 D_1 + b_2^2 D_2$$

D_1 and D_2 are the diffusion constants for the rotations about χ_2 and χ_3, respectively, and γ_1 is the amplitude of the restricted rotation about χ_2. β_{12} is the angle between the two rotation axes and β_{2F} is the angle between the second rotation axis and the C−H internuclear vector.

(2) Restricted rotational diffusion about χ_2 and χ_3. The spectral density function in this case is

$$J(\omega) = \sum_{n_1,n_2=0}^{\infty} \sum_{b_1,b_2,b_2'=-2}^{2} d^{(2)}_{b_1b_2}(\beta_{12}) d^{(2)}_{b_1b_2'}(\beta_{12}) \times E(b_1,n_1)^2 d^{(2)}_{b_20}(\beta_{2F}) d^{(2)}_{b_2'0}(\beta_{2F}) E(b_2,n_2) E(b_2',n_2) \times \mathrm{Re}\left[\frac{1}{(\alpha' + i\beta')^{1/2}}\right] \qquad (13)$$

α' and β' are obtained by replacing τ_0^{-1} in eqs 5 and 6 by

$$\tau_0^{-1} + \left(\frac{n_1\pi}{2\gamma_1}\right)^2 D_1 + \left(\frac{n_2\pi}{2\gamma_2}\right)^2 D_2$$

Here, γ_2 is the amplitude of the restricted rotation about χ_3.

In the calculations, we have assumed a tetrahedral arrangement of the side groups and the angle between the rotational axes (denoted as β) was taken as 70.5°. The optimized structure obtained from AM1 calculation for the model compound shows that the assumption is valid. In all these cases, the correlation times for internal rotations have been defined as $\tau_{ir} = (6D_i)^{-1}$.[19]

Numerical Calculations

Relaxation data were analyzed by using the spectral density functions described in the previous section. In order to obtain a fit of T_1 as a function of temperature, we have introduced the temperature dependence of correlation times in the spectral density expression.

Helfand[23] has applied Kramers'[24] theory for the diffusion of a particle over a potential barrier to conformational transitions in a polymer. According to this theory, the correlation time τ, for a conformational transition involving an energy barrier E_a, is written as

$$\tau = B\mathrm{e}^{E_a/RT} \qquad (14)$$

where $B = \eta c$, η being the viscosity and c, a molecular constant. In the calculations, the activation energy E_a and the pre-exponential factor, B, were taken as adjustable parameters. Glowinkowski et al.[25] have shown that the linear dependence of correlation time on viscosity is not observed when the time scales for the polymer and solvent motions are not cleanly separable; instead they have obtained a power law relationship between correlation time and viscosity. However, in

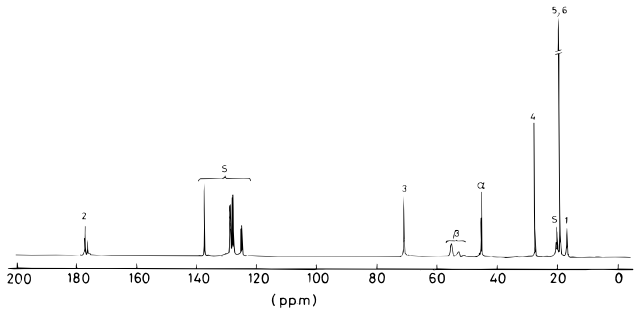

Figure 1. Proton-decoupled ^{13}C spectrum of poly(isobutyl methacrylate) in toluene-d_8 at 100.6 MHz. Solvent peaks are denoted S.

this study the experimental data show that the motional characteristics are far away from the extreme narrowing limit, implying that the polymer motion must be slow. Hence we assume that the use of eq 14 may not lead to very large errors.

The temperature dependent T_1 values at both frequencies were fitted simultaneously. The experimental T_1 values of the backbone methylene carbon at different temperatures were used as the input data. The parameters B, E_a, and f were included in the fitting procedure and the remaining parameters, namely, τ_0/τ_1 and τ_1/τ_l, were adjusted manually. The parameters obtained from the backbone data were held constant while obtaining the best fit to the side-chain T_1 values. In order to obtain the best fit to the relaxation data of the nuclei in the ester side chain, initially the parameters corresponding to χ_2 motion are varied to obtain the best fit to the T_1 values of C_3. These parameters are held constant while varying the parameters corresponding to χ_3 motion, to obtain the best fit to the C_4 T_1 values. The deviations between the calculated and experimental quantities are expressed as the mean square relative deviation denoted as d. The conformational energy calculations have been carried out by the AM1 method,[26] as implemented in the Gaussian 92 program package.[27]

Results

The ^{13}C spectrum of PIBM is shown in Figure 1. The peaks have been assigned by analogy with the reported ^{13}C spectra of poly(alkyl methacrylates)[28,29] and poly(alkyl acrylates).[30] The backbone methylene, quarternary, and carboxyl carbons show splittings arising from sensitivity to stereochemical configuration along the chain, and comparisons with spectra of related polymers show that these are typical of a syndiotactic polymer.

In Table 1, we summarize the ^{13}C T_1 and NOE values for the protonated carbons of PIBM. On examining the relaxation of the different components of the backbone methylene carbon resonance, the T_1 values were found to be independent of the stereosequences along the chain. The T_1 and NOE values reported here are for the low-field component of the methylene carbon resonance. Relaxation measurements were not carried out for C_5 and C_6 carbons since the signal overlaps with the solvent signal, especially at the lower magnetic field. An examination of the data reveals the following features. The T_1 values for the backbone carbon lie on the higher correlation time side of the T_1 minimum. With an increase of temperature, a minimum in the T_1 is observed for the backbone methylene carbon at the lower field. At the higher field, T_1 decreases with temperature and a minimum can be observed only at still higher temperatures. This is consistent with the fact that the T_1 minimum is shifted to higher temperatures with increasing field strength. The dependence of T_1 on the magnetic field in the entire temperature range of study and the fact that the NOE values are below the limiting value of 3.0 imply that the motional characteristics are far below the extreme narrowing limit.

The T_1 values of the side-chain carbons are higher than that of the backbone carbon. It suggests that the side chains have additional mobility arising from internal rotation. The T_1 values for the C_1 carbon increases with temperature, and at higher temperatures the values are higher than that of the backbone carbon. This is clearly evident from the data at lower field. In the case of the C_3 carbon of the ester side chain, the T_1 value passes through a minimum with an increase in temperature. For the C_4 carbon, the T_1 value increases with temperature and they are higher than that of the T_1 values of C_3. Such an increase in the T_1 values of successive carbons has been observed in alkyl chains attached to a macromolecule.[29,31,32] This increase results from the greater mobility of the alkyl chain toward its free end. The NOE values for the side chain carbons are below the limiting value of 3.0. All carbons with the exception of C_4 show a higher value of NOE at lower temperatures. With an increase in temperature, the NOE values first decrease and then increase. Such a behavior is observed when the overall motion of the backbone is slow and other motional modes, for example, side-chain rotations, become important in governing the relaxation process.[8,19]

Discussion

In modeling the dynamics of PIBM, we consider the following motions: (i) segmental rearrangements of the backbone, (ii) internal rotation of the α-methyl side group, and (iii) multiple internal rotations of the ester side group. Besides these, the overall tumbling of the polymer chain may also contribute to relaxation, especially if the correlation time is of the same order as that of the segmental motions or less. However, for high molecular weight polymers, the contribution to relaxation from overall tumbling becomes insignificant and hence we have not included it in the present analysis.[1,2]

Table 1. Experimental Carbon-13 Spin−Lattice Relaxation Times (ms) and NOE[a] of Protonated Carbons of PIBM as a Function of Temperature at Two Magnetic Fields

	backbone carbon		side-chain carbons					
	CH_2		C_1		C_3		C_4	
temp, K	50.3 MHz	100.6 MHz	50.3 MHz	100.6 MHz	50.3 MHz	100.6 MHz	50.3 MHz	100.6 MHz
296	81 (1.68)	192 (1.81)	53 (2.45)	89 (2.35)	147 (1.68)	336 (2.2)	293 (2.28)	407 (2.43)
313	73 (1.5)	172 (1.65)	68 (2.4)	103 (2.56)	138 (1.58)	314 (1.93)	378 (2.46)	518 (2.45)
333	67 (1.53)	139 (1.43)	101 (2.31)	110 (2.5)	144 (1.64)	241 (1.71)	542 (2.54)	663 (2.54)
343	67 (1.67)	128 (1.5)	118 (2.4)	135 (2.6)	164 (1.71)	254 (1.8)	711 (2.53)	839 (2.69)
353	71 (1.85)	120 (1.51)	132 (2.53)	157 (2.5)	194 (1.86)	269 (1.79)	878 (2.57)	1019 (2.68)

[a] Values in parentheses.

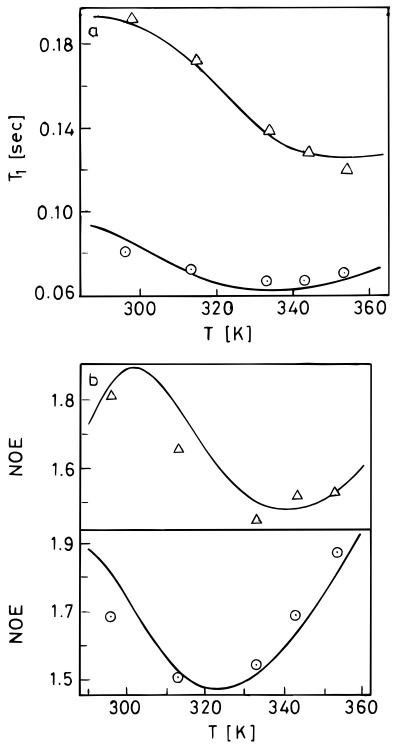

Figure 2. Temperature dependence of (a) T_1 and (b) NOE for the methylene carbon of PIBM in toluene-d_8 at field strengths of 100.6 (△) and 50.3 (⊙). The solid lines represent (a) the best fit values calculated by the DLM model and (b) the NOE predicted by the best fit of the DLM model.

Table 2. Simulation Parameters for the Methylene Carbon T_1 of PIBM Using the DLM Model

τ_0/τ_1	τ_1/τ_l	f	E_a, kJ/mol	$10^{14}A$, s	10^3d
2	50	0.36	36.4	0.739	1.79

In this study, we have used the DLM model to describe the backbone motion. For the description of the side-chain dynamics, we have utilized various motional models which describe internal rotations in the side chains. To gain further insight into the nature of internal rotations in the side chains, we have carried out conformational energy calculations using the semiempirical quantum chemical method AM1. These analyses are described in the following section.

(i) Segmental Motion of the Main Chain. Models which describe backbone motion in terms of conformational transitions occurring in short segments of a polymer chain have been found to be successful in reproducing the experimental T_1 versus temperature curve on the lower correlation time side of the T_1 minimum. However, recent studies have shown that a more rigorous test for the validity of a model is its ability to reproduce the experimentally observed T_1 minimum.[4−6,33−37] Models which include librations of the backbone C−H vectors, in addition to conformational transitions, have been found to be superior in this regard.

The best fit of T_1 versus temperature curves for the backbone carbon calculated on the basis of the DLM model is shown in Figure 2 and the corresponding model parameters are summarized in Table 2. A good fit is obtained in the entire temperature range. A rather small value of the ratio τ_0/τ_1 indicates that the single conformational transitions associated with damping play an important role in PIBM. It is of interest to compare the value of this ratio with those obtained for structurally related polymers. By using the DLM model to analyze the experimental results of Levy et al.[29] on poly(butyl methacrylate) (PBMA) and poly(hexyl methacrylate) (PHMA), Spyros and Dais[38] obtained a value of 5 for both the polymers. For poly(naphthyl acrylate) (PNA) and ratio obtained is 3. However, it increases for poly(naphthyl acrylates).[37] These observations suggest that a smaller value of this ratio implies decreased flexibility of the backbone. Among the polymers considered, in PNA and PIBM the steric crowding in the vicinity of the backbone should be greater; in the former it is caused by the presence of the bulky naphthyl group and in the latter due to chain branching in the ester side group.

From the parameters given in Table 2, it is seen that the librational motion is about 50 times faster than the segmental motion and it accounts for nearly 36% of the decay of the correlation function. The rather high value of f implies that the librational mode is significant in determining the relaxation of the backbone carbon. The amplitude of the librational motion can be estimated from the parameter f in conjunction with Howarth's restricted rotation model using the expression[39]

$$1 - f = \left[\frac{\cos\theta - \cos^3\theta}{2(1 - \cos\theta)}\right]^2 \qquad (15)$$

The librational motion is described as the motion of the C−H vector inside a cone of half-angle θ, the axis of the cone being the rest position of the C−H bond. In this case, the conic half-angle is estimated to be 30.5°.

The validity of a motional model can be tested further by examining its ability to predict other experimental quantities. The parameters which fit the T_1 data as a function of temperature should also be able to predict NOE as a function of temperature. The measured NOEs thus provide an independent source for testing the correlation function.[40] The parameters obtained by fitting the T_1 data were used to calculate NOE as a function of temperature for the backbone carbon, and the results are shown in Figure 2.

It is interesting to note that in the temperature range in which the measurements have been carried out, the NOE decreases, reaches a minimum, and then increases as the temperature increases. This observation cannot be explained by any model which describes backbone dynamics on the basis of a single motional mode. Unimodal functions predict NOE to be dependent on correlation time only in the region of the T_1 minimum. For higher correlation times, away from that of the T_1 minimum, the NOE approaches the lower asymptotic limit. The observed temperature dependence of NOE is reproduced satisfactorily by the DLM model, which considers the librational mode in addition to the conformational transition in its motional description. It is interesting to compare this situation with the models which describe relaxation behavior of nuclei in side groups attached to a molecule undergoing overall tumbling. The presence of side group rotation in addition to overall tumbling has been shown to result in an initial decrease of the NOE followed by an increase in cases where the correlation time for overall tumbling falls on the higher correlation time side of the T_1 minimum.[19] The ability to reproduce the temperature dependence of NOE in the high correlation time region further demonstrates the importance of including the librational mode for a better description of the backbone motion. The experimental work by Levy et al.[29] on PBMA and

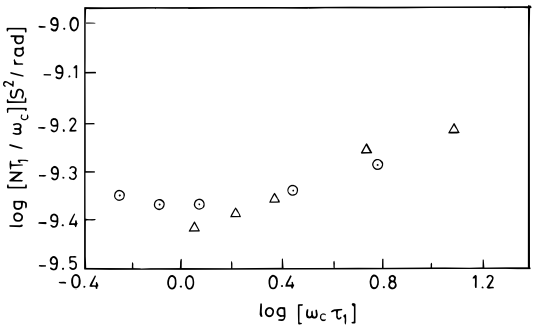

Figure 3. Frequency−temperature superposition of ^{13}C NMR NT_1 values for the backbone methylene carbon of PIBM in toluene-d_8. τ_1 values are the correlation times obtained from the analysis of the relaxation data by using the DLM model. Larmor frequencies are 100.6 MHz (△) and 50.3 MHz (⊙).

PHMA reports NOE measurements in the high correlation time region, and recent analysis of the results by Spyros and Dais[38] has shown that the DLM function is superior to unimodal distribution (log χ^2) in reproducing the observed NOEs.

Guillermo et al.[41] have proposed a method for superimposing NT_1 data obtained at different Larmor frequencies. This superposition is possible only if the molecular motions that are considered in the correlation function are governed by a single basic correlation time $\tau(T)$. A plot of $\log(NT_1/\omega_C)$ versus $\log(\omega_C\tau_1)$ shown in Figure 3 indicates that the ^{13}C relaxation data at the two Larmor frequencies superposes fairly well. The success of the superposition implies that the mechanisms of local motions as reflected in the correlation function are independent of temperature, and it justifies the attempts to fit the data to a correlation function whose shape is independent of temperature.

Fitting of the experimental data to the DLM model yields an apparent activation energy of 36.4 kJ/mol. This high value might result from the presence of bulky substituents on the chain backbone and it is comparable to the value of 33 kJ/mol observed in the case of PHMA.[38] This high value seems to imply reduced flexibility of the chain, which is to be expected due to the presence of the branched side chain which can cause steric hindrance to the conformational transitions along the chain backbone. Earlier studies on poly(alkyl methacrylates) have also led to the conclusion that chain segmental mobility decreases with an increase in the bulkiness of the ester group.[42]

(ii) Internal Rotation of the α-Methyl Side Group. The relaxation of the methyl carbon reflects conformational transitions along the chain backbone as well as rotation of the methyl group. We have analyzed the relaxation behavior of the C_1 carbon by considering three different motional models for methyl rotation, namely, unrestricted rotational diffusion, the three site jump model with equal populations and jump rates, and restricted rotational diffusion. The last model has been considered in order to examine the possibility of a restricted motion which might occur due to the presence of bulky substituents.

In their analysis of the relaxation of methyl side groups in poly(methyl methacrylate) and poly(isobutylene), Heatley et al.[43,44] have considered the methyl group internal rotation to be dependent on the backbone motion. We have assumed that the backbone motion and methyl rotation are independent since the experimental T_1 values for the backbone carbon fall on the higher side of the correlation time of the T_1 minimum

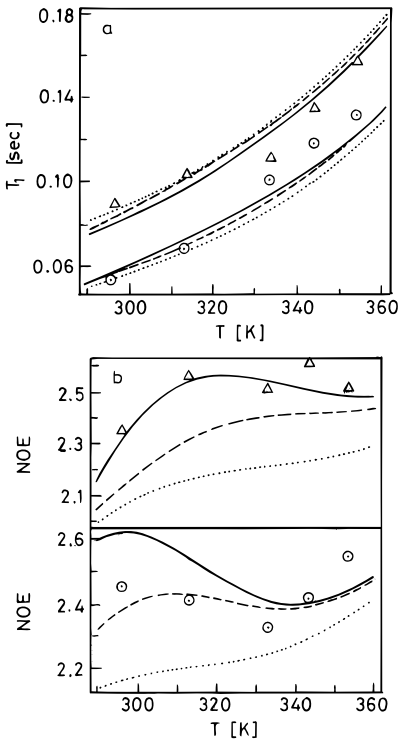

Figure 4. Temperature dependence of (a) T_1 and (b) NOE for the C_1 carbon of PIBM in toluene-d_8 at field strengths of 100.6 (△) and 50.3 MHz (⊙). The solid, dashed, and dotted lines represent (a) the best fit values calculated by the three site jump model, unrestricted rotational diffusion model, and restricted rotational diffusion model, respectively, and (b) the NOE predicted by the best fit of the corresponding models.

Table 3. Simulation Parameters for C_1 T_1

models for χ_1 motion	E_a, kJ/mol	$10^{14}A$, s	C	10^3d
unrestricted rotational diffusion	23.3	1.057		6.86
three site jump	20.6	7.613		6.25
restricted rotational diffusion	27.4	0.179	10.8	10.6

whereas they are on the lower correlation time side for C_1. This suggests that the time scales for these motions must be well separated and the motions could be treated independently.

The best fit T_1 versus temperature curves for the C_1 carbon based on the three models are shown in Figure 4, and the corresponding model parameters are given in Table 3. For the restricted rotation model, the temperature dependence of the rotational amplitude was assumed to be of the form[12]

$$\alpha = CT^{1/2} \tag{16}$$

The curves calculated using the unrestricted rotation model and the threesite jump model are closer to the experimental values. The restricted rotation model on the other hand shows a larger deviation from the experiment. Using the restricted rotation model, the best fit is obtained for rotational amplitudes ranging from 186 to 203° as the temperature increases from 296 to 353 K. The apparent activation energy for the methyl group motion, estimated from the unrestricted rotation model and three site jump model are comparable whereas the restricted rotation model yields a higher barrier.

The NOE data as a function of temperature, as predicted by the parameters which give the best fit to the T_1 data, are shown in Figure 4. Among the three

models considered, the three site jump model is the closest to the experimental values. Even though the deviation from the experimental values is slightly higher at the lower field, the predicted values are within experimental error. For the calculations based on the three site jump models the mean square relative deviation estimated for the NOE data at both fields is 1.37×10^{-3}. The validity of the three site jump model in describing methyl group motion is supported by conformational energy calculations.

(iii) Multiple Internal Rotations of the Ester Side Group. In modeling the dynamics of the ester side group, we consider rotations about the O−C_3 bond (χ_2 motion) and C_3−C_4 bond (χ_3 motion). These motions are assumed to be independent. It is important to note that additional flexibility within the ester group, namely, rotations about the C_α−C_2 and C_2−O bonds, can affect the rate of side chain motion. Of these, the rotation about the C_2−O bond can be neglected because conjugation effects can lead to very high energy barriers. The rotation of the C_α−C_2 bond, that is, the rotation of the alkoxy group as a whole, has been studied theoretically.[45,46] Besides, this rotation is believed to result in β-relaxation observed in dielectric and mechanical loss experiments.[47] The experimentally observed activation energy for the β-relaxation is found to be in the range 70−95 kJ/mol for poly(alkyl methacrylates). From molecular mechanics calculations in which torsional deformation of the main chain is allowed, Heijboer et al.[46] obtained a value of 30 kJ/mol for the barrier for the alkoxycarbonyl group rotation. On constraining the torsional angles of the main chain, they obtained a value of 69 kJ/mol. Cowie and Ferguson[45] in their molecular mechanics study of the same process obtained values in the range 70−90 kJ/mol by assuming this to be a localized motion so that a majority of the neighboring atoms are rigid and only relatively few spatial readjustments of selected atoms are allowed to take place. From relaxation studies carried out in solution for poly(naphthylalkyl acrylates) Spyros et al.[37] estimated the energy barrier for this rotation to be 20 kJ/mol.

On the basis of these observations, it is rather difficult to arrive at a definite conclusion regarding the energy barrier for the alkoxycarbonyl group rotation. It is possible that in solution, there is considerable flexibility about this bond; however, from the present experimental data, it is not possible to carry out an effective analysis of the possible motions within the alkoxycarbonyl group.

In the present work, we consider two models for the internal rotation in the ester side chain; one in which the χ_2 motion is a restricted rotational diffusion and the χ_3 motion is an unrestricted rotational diffusion. In the second, we model both χ_2 and χ_3 motions as restricted rotational diffusion. The assumption of an unrestricted rotation about the O−C_3 bond (χ_2 motion) leads to unreasonable values for the parameters. In the fitting procedure, we have assumed the temperature dependence of the rotational amplitudes to be of the form given in eq 16.

The best fit T_1 versus temperature curves and the predicted NOE versus temperature curves for the C_3 carbon are shown in Figure 5, and the corresponding model parameters are given in Table 4. By assuming a restricted rotation model for the χ_2 motion, it is possible to reproduce the observed trends in T_1 and NOE fairly well, and most of the calculated values fall within the experimental error. The predicted NOE values at the lower field are slightly higher than the experimental values at all temperatures.

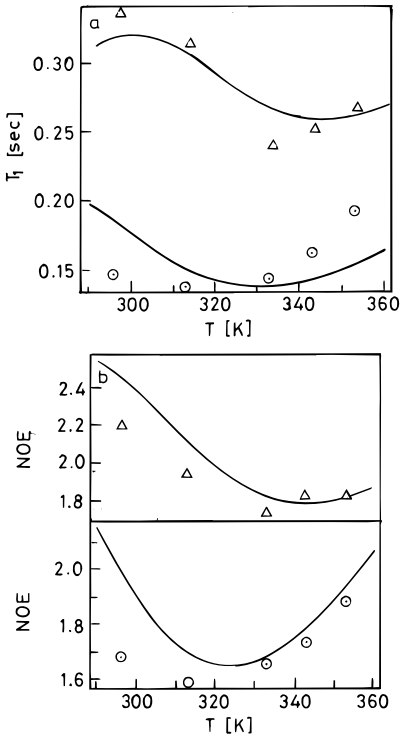

Figure 5. Temperature dependence of (a) T_1 and (b) NOE for the C_3 carbon of PIBM in toluene-d_8 at field strengths of 100.6 (△) and 50.3 MHz (⊙). The solid lines represent (a) the best fit values calculated by the restricted rotational diffusion model and (b) the NOE predicted by the best fit of the restricted rotational diffusion model.

Figure 6 shows the best fit T_1 versus temperature curves for the C_4 carbon, and the model parameters are included in Table 4. Both unrestricted and restricted rotation models for χ_3 motion give a good fit to the T_1 values. The parameters which give the best fit to the T_1 values have been utilized to predict NOE as a function of temperature, and the results are shown in Figure 6. The mean square relative deviation in the predicted NOE is lower for the restricted rotation model. Even though most of the calculated NOE values fall within experimental error, the prediction is not entirely satisfactory because the predicted NOEs are higher than the experimental values at all temperatures in the lower field.

In Table 5 we summarize the diffusion constants and rotational amplitudes for χ_2 and χ_3 motions. The diffusion constant is higher for χ_2 motion. A similar situation has been observed by Spyros and Dais[38] for PBMA, and they have interpreted it on the basis of cumulative bond rotations within the ester group, which affect the relaxation of the first carbon in the chain. A comparison of the rotational amplitudes for the two motions shows that the rotation is more restricted about the O−C_3 bond. For rotation about the C_3−C_4 bond, we obtain large rotational amplitudes. This is probably because, as one approaches the chain end, it is not unreasonable to assume free rotation about the bond. In PIBM we have a branched alkyl chain and the C_3−C_4 bond is effectively the chain end.

Interesting comparison can be made between solution dynamics and relaxations observed for the bulk polymers by other experimental methods. The δ relaxation observed by dielectric and mechanical loss experiments is believed to result from internal motions within the

Table 4. Simulation Parameters for Ester Side-Chain Carbons

	parameters for C_3 T_1					parameters for C_4 T_1			
models for χ_2 motion	E_a, kJ/mol	$10^{14}A$, s	C	10^3d	models for χ_3 motion	E_a, kJ/mol	$10^{14}A$, s	C	10^3d
restricted rotational diffusion	16.9	2.778	4.5	15.2	unrestricted rotational diffusion	25.4	0.543		2.71
					restricted rotational diffusion	31.0	0.086	8.2	1.79

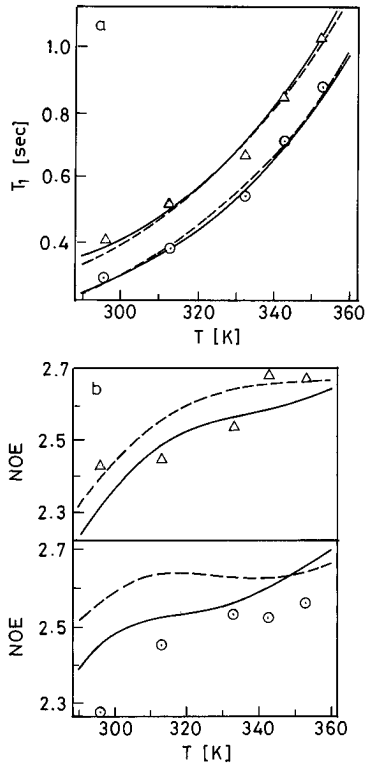

Figure 6. Temperature dependence of (a) T_1 and (b) NOE for the C_3 carbon of PIBM in toluene-d_8 at field strengths of 100.6 (△) and 50.3 MHz (⊙). The solid and dashed lines represent (a) the best fit values calculated by the restricted rotational diffusion model and unrestricted rotational diffusion model, respectively, and (b) the NOE predicted by the best fit of the corresponding models.

Table 5. Diffusion Constants and Rotational Amplitude for χ_2 and χ_3 Motions

	χ_2 motion		χ_3 motion	
temp, K	$10^{-9}D_1$, s^{-1}	γ_1	$10^{-9}D_2$, s^{-1}	γ_2
296	6.13	77.4	0.65	141.1
313	8.92	79.6	1.30	145.1
333	13.19	82.1	2.65	149.6
343	15.75	83.3	3.67	151.8
353	18.65	84.5	4.50	154.1

ester side group. Shimizu et al.[48] have carried out dielectric relaxation studies of the δ relaxation in a series of poly(alkyl methacrylates). Ochiai et al.[49] have studied this process by dynamic mechanical measurements. Both groups conclude that the motional process involved in δ relaxation in PIBM is the rotation of the isopropyl group at the end of the ester side chain. Our observation of a highly restricted motion about the $O-C_3$ bond and a greater rotational freedom about the C_3-C_4 bond is consistent with these results.

Conformational Energy Calculations

In order to obtain further insight into the nature of the side group motions, we have carried out conformational energy calculations using the semiempirical quantum chemical method AM1.[26] An independent estimate of the activation barriers for the rotations about the various bonds will also help to check the validity of the various models used to describe side-chain dynamics.

The conformational energy calculations were carried out on the following model which was chosen to represent the polymer under investigation.

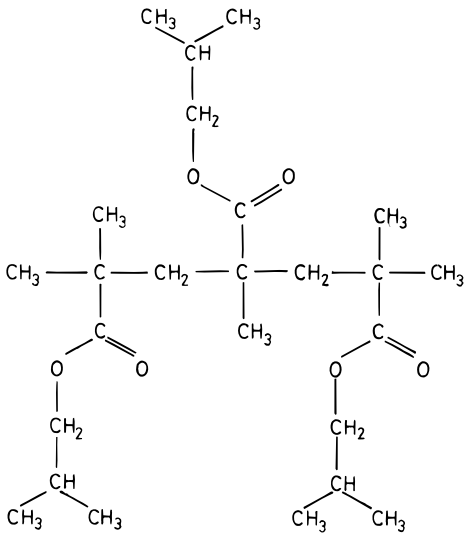

Initially, the structure of the model compound was fully optimized. The optimized structure was found to have an all-trans conformation for the backbone and a tetrahedral arrangement about the carbon atoms of the side chains. The potential energy curves were calculated for the rotation of the methyl side chain and the isobutyl and isopropyl side groups of the ester side chain. The calculations were made for the side groups on the central carbon atom. In order to generate the potential energy curve, we begin from the optimized structure and perform the rotation about the concerned bond in steps of 10°. At each step, all the bond angles and torsional angles were optimized in order to avoid a possible overestimation of the potential barrier of interest. The bond lengths, however, were kept constant, since it is very unlikely that the bond length changes appreciably as a result of the side-chain rotations.

The relative potential energy as a function of the rotation angle (ϕ), for the rotation of the methyl side group is given in Figure 7. The potential energy curve is symmetrical and shows a 3-fold barrier. The energy barrier is 12.4 kJ/mol. It is interesting to note that among the models considered for describing methyl group rotation, the three site jump model is the most satisfactory one.

Figure 7 shows the relative potential energy as a function of the rotation angle, for the rotation of the isobutyl group of the ester side chain. It is clear that a full rotation involves an excessively high energy barrier of about 42 kJ/mol. Because of the steep energy barrier, only fluctuations of the order of 80° can occur about this bond. It is to be noted that the unrestricted rotational diffusion model was found unsuitable to describe the χ_2 motion. A satisfactory fit to the experimental data was

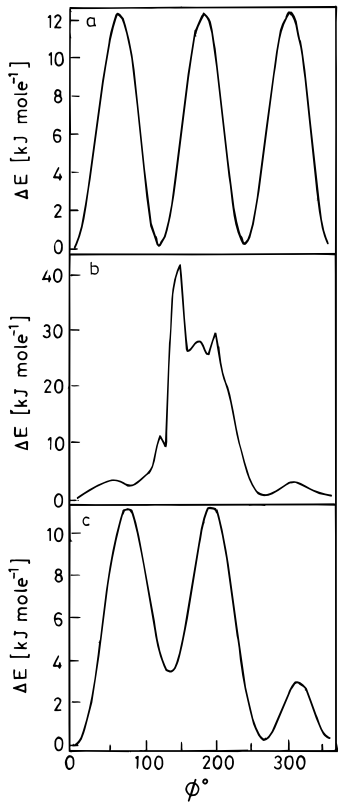

Figure 7. Energy barriers for (a) χ_1 motion, (b) χ_2 motion, and (c) χ_3 motion calculated using the semiempirical quantum chemical method, AM1.

obtained by describing the χ_2 motion as a restricted rotation. Interestingly, in the temperature range 296−363 K, the rotational amplitude estimated from the relaxation data falls in the range 77−85°. This is consistent with the results of the AM1 calculation.

The relative potential energy as a function of the rotation angle, for the rotation of the isopropyl group in the ester side chain is shown in Figure 7. A complete rotation involves three barriers, two of which are equal. The energy barriers involved are very low, of the order of 11 kJ/mol. At ambient temperatures, these energy barriers are overcome so readily that essentially a free rotation can occur. In the analysis of the experimental data we observe that both unrestricted and restricted rotation models are able to account for the results fairly well. In fact, the rotational amplitudes estimated using the restricted rotation model are rather high, indicating considerable rotational freedom for the isopropyl group.

Conclusions

The ^{13}C relaxation data for the backbone methylene carbon of PIBM have been analyzed by the DLM model. The DLM model yields a good fit to the experimental T_1 data and satisfactorily reproduces the NOE behavior. Different motional models have been utilized to analyze the relaxation data of the side-chain carbons. The α-methyl side-chain data was analyzed in terms of the unrestricted rotational diffusion model, three site jump model, and restricted rotational diffusion model. While the last model gave a poor fit to the experimental T_1 data, the remaining two models gave similar fits. However, in predicting the behavior of NOE, the three site jump model was more satisfactory. The multiple internal rotation model has been used to analyze the relaxation data of the ester side chain. Only the restricted rotational diffusion model could reproduce the relaxation data of the C_3 carbon. In the analysis of the relaxation data of the C_4 carbon, we have considered both restricted rotational diffusion and unrestricted rotational diffusion about the C_3-C_4 bond. The performances of the two models are similar. However, the rather large rotational amplitudes obtained by using the restricted rotation model indicate a relatively high degree of rotational freedom about the C_3-C_4 bond. The conformational energy calculations carried out on a model compound confirm the validity of the models used in describing the side-chain motions.

Acknowledgment. The 400 MHz NMR experiments were carried out at the Sophisticated Instruments Facility, Indian Institute of Science. We thank the staff for assistance. S.R. is grateful to the Council of Scientific and Industrial Research (CSIR), India, for a fellowship.

References and Notes

(1) Heatley, F. In *Dynamics of Chain in Solution by NMR Spectroscopy*; Booth, C., Price, C., Eds.; Comprehensive Polymer Science; Pergamon Press: New York, 1990; Vol. 18, p 377.
(2) Heatley, F. *Prog. Nucl. Magn. Reson. Spectrosc.* **1979**, *13*, 47.
(3) Heatley, F. *Annu. Rep. NMR Spectrosc.* **1986**, *17*, 179.
(4) Dejean de la batie, R.; Laupretre, F.; Monnerie, L. *Macromolecules* **1988**, *21*, 2045.
(5) Gisser, D. J.; Glowinkowski, S.; Ediger, M. D. *Macromolecules* **1991**, *24*, 4270.
(6) Ravindranathan, S.; Sathyanarayana, D. N. *Macromolecules* **1995**, *28*, 2396.
(7) Levine, Y. K.; Partington, P.; Roberts, G. C. K. *Mol. Phys.* **1973**, *25*, 497.
(8) London, R. E.; Avitabile, J. *J. Chem. Phys.* **1976**, *65*, 2443.
(9) Wallach, D. *J. Chem. Phys.* **1967**, *47*, 5258.
(10) Wittebort, R. J.; Szabo, A. *J. Chem. Phys.* **1978**, *69*, 1722.
(11) London, R. E.; Avitabile, J. *J. Am. Chem. Soc.* **1978**, *100*, 7159.
(12) Gronski, W.; Murayama, N. *Makromol. Chem.* **1978**, *179*, 1521.
(13) Woessner, D. E. *J. Chem. Phys.* **1962**, *1*, 36.
(14) Tsutsumi, A. *Mol. Phys.* **1979**, *37*, 111.
(15) London, R. E.; Avitabile, J. *J. Am. Chem. Soc.* **1977**, *99*, 7765.
(16) We have used a relatively high concentration, in order to obtain a better signal to noise ratio for the methylene carbon of the chain backbone.
(17) Sass, M.; Ziessow, D. *J. Magn. Reson.* **1977**, *25*, 263.
(18) Levy, G. C.; Peat, I. R. *J. Magn. Reson.* **1975**, *18*, 500.
(19) Doddrell, D.; Glushko, V.; Allerhand, A. *J. Chem. Phys.* **1972**, *56*, 3683.
(20) Pople, J. A.; Gordan, M. S. *J. Am. Chem. Soc.* **1967**, *89*, 4253.
(21) Hall, C. K.; Helfand, E. *J. Chem. Phys.* **1982**, *77*, 3275.
(22) Rose, M. E. *Elementary Theory of Angular Momentum*: Wiley: New York, 1957.
(23) Helfand, E. *J. Chem. Phys.* **1971**, *54*, 4651.
(24) Kramers, H. A. *Physica* **1940**, *7*, 284.
(25) Glowinkowski, S.; Gisser, D. J.; Ediger, M. D. *Macromolecules* **1990**, *23*, 3520.
(26) Dewar, M. J. S.; Zoebisch, E. G.; Healy, E. J. *J. Am. Chem. Soc.* **1985**, *107*, 3902.
(27) Frisch, M. J.; Trucks, G. W.; Head-Gordon, M.; Gill, P. M. W.; Wong, M. W.; Foresman, J. B.; Johnson, B. G.; Schlegel, H. B.; Robb, M. A.; Replogle, E. S.; Gomperts, R.; Andreas, J. L.; Raghavachari, K.; Binkley, J. S.; Gonzalez, C.; Martin, R. L.; Fox, D. J.; Baker, J.; Stewart, J. J. P.; Pople, J. A. Gaussian 92, Revision E. 3; Gaussian Inc.: Pittsburg, PA, 1992.
(28) Lyerla, J. R.; Horikawa, T. T.; Johnson, D. E. *J. Am. Chem. Soc.* **1977**, *99*, 2463.
(29) Levy, G. C.; Axelson, D. E.; Schwartz, R.; Hochmann, J. *J. Am. Chem. Soc.* **1978**, *100*, 410.
(30) Matsuzaki, K.; Kanai, T.; Kawamura, T.; Matsumoto, S.; Uryu, T. *J. Polym. Sci., Polym. Phys. Ed.* **1973**, *11*, 961.
(31) Ghesquiere, D.; Chachaty, C.; Tsutsumi, A. *Macromolecules* **1979**, *12*, 775.
(32) Spyros, A.; Dais, P.; Marchessault, R. H. *J. Polym. Sci., Polym. Phys. Ed.* **1995**, *33*, 367.

(33) Dejean de la Batie, R.; Laupretre, F.; Monnerie, L. *Macromolecules* **1988**, *21*, 2052.
(34) Dejean de la Batie, R.; Laupretre, F.; Monnerie, L. *Macromolecules* **1989**, *22*, 122.
(35) Dejean de la Batie, R.; Laupretre, F.; Monnerie, L. *Macromolecules* **1989**, *22*, 2617.
(36) Radiotis, T.; Brown, G. R.; Dais, P. *Macromolecules* **1993**, *26*, 1445.
(37) Spyros, A.; Dais, P.; Heatley, F. *Macromolecules* **1994**, *27*, 5845.
(38) Spyros, A.; Dais, P. *J. Polym. Sci., Polym. Phys. Ed.* **1995**, *33*, 353.
(39) Howarth, O. W. *J. Chem. Soc., Faraday Trans. 2* **1979**, *75*, 863.
(40) Denault, J.; Prud'homme, J. *Macromolecules* **1989**, *22*, 1307.
(41) Guillermo, A.; Dupeyre, R.; Cohen-Addad, J. P. *Macromolecules* **1990**, *23*, 1291.
(42) Hatada, K.; Kitayama, T.; Ute, K. *Annu. Rep. NMR. Spectrosc.* **1993**, *26*, 99.
(43) Heatley, F.; Begum, A. *Polymer* **1976**, *17*, 399.
(44) Heatley, F. *Polymer* **1975**, *16*, 493.
(45) Cowie, J. M. G.; Ferguson, R. *Polymer* **1987**, *28*, 503.
(46) Heijboer, J.; Baas, J. M. A.; van de Graaf, B.; Hoefnagel, M. A. *Polymer* **1987**, *28*, 509.
(47) McCrum, N. G.; Read, B. E.; Williams, G. *Anelastic and Dielectric effects in Polymeric Solids*; John Wiley: London, 1967.
(48) Shimizu, K.; Yano, O.; Wada, Y. *J. Polym. Sci., Polym. Phys. Ed.* **1975**, *13*, 1959.
(49) Ochiai, H.; Shindo, H.; Yamamura, H. *J. Polym. Sci., Polym. Phys. Ed.* **1971**, *9*, 431.

MA951207T